


Impact of calcification on Murray law-based quantitative flow ratio for physiological assessment of intermediate coronary stenoses

Wenjie Zuo^{1*}, Renhua Sun^{2*}, Yang Xu^{1*}, Zhenjun Ji¹, Rui Zhang¹,
Xiaoguo Zhang¹, Shengxian Tu³, Genshan Ma¹

¹Department of Cardiology, Zhongda Hospital, School of Medicine, Southeast University, Nanjing, China

²Department of Cardiology, The First People's Hospital of Yancheng, Yancheng, China

³Med-X Research Institute, School of Biomedical Engineering,
Shanghai Jiao Tong University, Shanghai, China

Abstract

Background: To investigate the influence of coronary calcification on the diagnostic performance of Murray law-based quantitative flow ratio (μ QFR) in identifying hemodynamically significant coronary lesions referenced to fractional flow reserve (FFR).

Methods: A total of 571 intermediate lesions from 534 consecutive patients (66.1 ± 10.0 years, 67.2% males) who underwent coronary angiography and simultaneous FFR measurement were included. Calcific deposits were graded by angiography as none or mild (spots), moderate (involving $\leq 50\%$ of the reference vessel diameter), and severe ($> 50\%$). Performance of μ QFR to detect functional ischemia ($FFR \leq 0.80$) was evaluated, including diagnostic parameters and areas under the receiver-operating curves (AUCs).

Results: The discrimination of ischemia by μ QFR was comparable between none/mild and moderate/severe calcification (AUC: 0.91, 95% confidence interval: 0.88–0.93 vs. AUC: 0.87, 95% confidence interval: 0.78–0.94; $p = 0.442$). No statistically significant difference was observed for μ QFR between the two categories in sensitivity (0.70 vs. 0.69, $p = 0.861$) and specificity (0.94 vs. 0.90, $p = 0.192$). Moreover, μ QFR showed significantly higher AUCs than quantitative coronary angiographic diameter stenosis in both vessels with none/mild (0.91 vs. 0.78, $p < 0.001$) and moderate/severe calcification (0.87 vs. 0.69, $p < 0.001$). By multivariable analysis, there was no association between calcification and μ QFR-FFR discordance (adjusted odds ratio: 1.529, 95% confidence interval: 0.788–2.968, $p = 0.210$) after adjustment for other confounding factors.

Conclusions: Murray law-based quantitative flow ratio demonstrated robust and superior diagnostic performance for lesion-specific ischemia compared with angiography alone regardless of coronary calcification. (Cardiol J 2024; 31, 2: 205–214)

Keywords: calcification, fractional flow reserve, coronary artery disease, diagnosis, quantitative flow ratio

Address for correspondence: Genshan Ma, MD, PhD, FACC, Department of Cardiology, Zhongda Hospital, School of Medicine, Southeast University, No. 87 Dingjiaqiao, Nanjing 210009, China, e-mail: magenshan@seu.edu.cn

*These authors contributed equally to this work.

Received: 15.08.2022

Accepted: 15.06.2023

Early publication date: 30.06.2023

This article is available in open access under Creative Commons Attribution-Non-Commercial-No Derivatives 4.0 International (CC BY-NC-ND 4.0) license, allowing to download articles and share them with others as long as they credit the authors and the publisher, but without permission to change them in any way or use them commercially.

Introduction

Although fractional flow reserve (FFR) has been shown as an effective tool in guiding revascularization to improve clinical outcomes and life quality in patients with stable coronary artery disease, it was underutilized in clinical practice mainly due to prolonged procedure time, increased medical expenses, and vasodilation-induced discomfort [1–3]. To overcome these limitations, several methods were developed based on computational fluid dynamics to simulate coronary artery flow without the requirement of any pressure wire or hyperemic agent [4]. Of these, angiography-derived quantitative flow ratio (QFR) was demonstrated to have good diagnostic performance for detecting lesion-specific ischemia, superior to conventional diameter stenosis, in recent multicenter trials using invasive FFR as the reference standard [5–7]. However, this technique requires two optimal angiographic images from at least 25 degrees apart, which is not always available in routine cardiac catheterization. Moreover, its accuracy might be influenced by individual variations in a semi-automatic drawing of vessel contour and frame counting.

Recently, an updated algorithm called Murry law-based QFR (μ QFR) has been proposed for functional evaluation of coronary stenosis severity [8]. This artificial intelligence (AI)-assisted approach could realize one-stop automatic hemodynamic assessment from a single angiographic view, which greatly simplifies the calculation process and reduces the amount of manual handling. A recent post hoc analysis of 306 patients in the FAVOR (Functional Diagnostic Accuracy of Quantitative Flow Ratio in Online Assessment of Coronary Stenosis) II China study has demonstrated its excellent correlation and agreement with FFR [8]. Despite the good performance of μ QFR in the overall population, the effect of coronary calcification on imaging-derived non-hyperemic physiological assessment was not fully addressed. In this study, it was sought to evaluate the diagnostic accuracy of μ QFR in vessels with different degrees of calcification and to compare μ QFR versus angiography alone in identifying the physiological significance of calcified and non-calcified coronary arteries with invasive FFR as the reference standard.

Methods

Study population

Electronic medical records between December 2012 and April 2021 were initially screened from

consecutive patients with coronary artery disease and at least one intermediate lesion by visual estimation (30–70% diameter stenosis) who underwent coronary angiography and simultaneous FFR measurements at the documented institution. Exclusion criteria were as follows: left-main disease, acute myocardial infarction within 72 hours, presence of myocardial bridge, in-stent restenosis in the interrogated vessel, insufficient image quality for QFR computation, and severe overlap of vessels by angiography. This study was approved by the institutional ethics committee of Zhongda Hospital and the requirement of informed consent was waived due to the retrospective manner.

Coronary angiography and FFR measurement

All patients received coronary angiography via the radial artery using a 5-French or 6-French system. Angiographic datasets were acquired at 15 frames/s using a monoplanar radiographic system (AXIOM Artis, Siemens, Erlangen, Germany). The severity of calcification was determined based on angiography as described by Karacsonyi et al. [9]: none or mild (spotty calcification), moderate (involving $\leq 50\%$ of the reference vessel diameter), and severe calcification (involving $> 50\%$ of the reference vessel diameter). After the assessment was completed by an experienced analyst (Dr. Xiaoguo Zhang), 20% of the images were randomly selected from each type of calcification and re-evaluated by another interventionalist (Dr. Renhua Sun). A strong inter-observer agreement was confirmed by a weighted kappa coefficient of 0.897 (95% confidence interval [CI]: 0.775–1.019, $p < 0.001$).

A 0.014-inch pressure guidewire (Certus, St. Jude Medical, St. Paul, Minnesota, USA) was equalized to the aortic pressure before being positioned distal to the lesion. Maximum hyperemia was induced by intravenous infusion of adenosine-5'-triphosphate (ATP) at $140 \mu\text{g/kg/min}$ for at least 2 minutes. During the steady phase of maximum hyperemia, the FFR value was calculated as the ratio of mean distal coronary pressure (Pd) to simultaneous mean aortic pressure (Pa). The threshold was defined as $\text{FFR} \leq 0.80$ to indicate functional ischemia [1]. The details of the procedure have been described in our previous reports [10, 11].

μ QFR computation and quantitative analysis

Offline computation of μ QFR was performed using commercial software (AngioPlus Core, Shanghai Pulse Medical Technology Inc., Shanghai,

China) by a certified analyst (Dr. Xiaoguo Zhang) who was blinded to patient characteristics and FFR information. The details of μ QFR analysis and its good repeatability have been described previously [8]. From an optimal angiographic view with minimal vessel overlap, contrast flow velocity was calculated and a keyframe with sharp lumen contour at the stenotic segment was selected for subsequent analysis. The delineation of the lumen contour and reconstruction of the reference diameter function was then performed by AI algorithms according to the Murray fractal law. Proximal and distal reference vessel diameters were corrected manually when needed. Ultimately, μ QFR values were obtained for both major epicardial arteries and their side branches. Parameters of quantitative coronary angiography (QCA) were also available from the software simultaneously, including diameter stenosis (QCA-DS), lesion length, and minimal lumen diameter.

Statistical analysis

The normality of quantitative data was examined using histograms and Q-Q plots. Continuous variables were expressed as mean \pm standard deviation or median with interquartile range and were compared using the Student t-test or Mann-Whitney U test as appropriate. Categorical variables were expressed as counts (percentages) and were compared using the chi-square test. The association and agreement between μ QFR and invasive FFR were analyzed by the Spearman's correlation coefficients and the Bland-Altman plots, respectively. The correlation coefficients were compared using a z-test on Fisher z transformation [12]. Diagnostic variables of μ QFR and QCA-DS to detect functionally significant lesions were assessed on a per-vessel level across different calcification subgroups. The "N-1" chi-square test was used for comparing these variables of μ QFR between the two calcification subgroups [13]. Receiver-operating characteristics curves were used for μ QFR and angiographic parameters to measure their discriminatory powers for identifying lesion-specific ischemia with invasive FFR as the reference standard. The area under the curves (AUCs) was compared according to the method by DeLong et al. [14]. Multivariate logistic regression was used to exclude the influence of confounding factors on the relationship between calcification and μ QFR-FFR discordance. All statistical analyses were performed with SPSS version 25.0 (IBM Corp., Armonk, New York, USA), Stata/SE 15.0 (StataCorp, College Station, TX, USA), GraphPad

Prism version 8.2.1 for macOS (GraphPad Software, San Diego, California, USA), and MedCalc® Statistical Software version 20.022 (MedCalc Software bvba, Ostend, Belgium). A two-tailed p-value < 0.05 was considered statistically significant.

Results

Patient and lesion characteristics

The flow diagram of patient selection is shown in Figure 1. Of the 677 patients initially screened, 534 patients (mean age 66.1 ± 10.0 years, 67.2% males) with 571 de novo lesions were eventually available for this analysis. Forty-six (8.6%) patients had a previous history of myocardial infarction and 461 (86.3%) patients presented stable angina. The average QCA-DS was $38.0 \pm 8.3\%$ and there were 387 (67.8%) lesions located in the left descending artery. The mean FFR was 0.85 ± 0.08 , with 150 (26.3%) vessels being physiologically significant ($\text{FFR} \leq 0.80$).

There were 496 (86.9%) lesions with no or mild calcification, 46 (8.1%) lesions with moderate calcification, and 29 (5.1%) lesions with severe calcification. Compared with those with no or mild calcification, patients with moderate or severe calcification were older and had a lower body mass index with less prevalence of single-vessel disease (Table 1). Moderately or severely calcified lesions were more likely to be located in the left anterior descending artery with a higher degree of QCA-DS, longer length, lower FFR, and μ QFR (Table 2). The distribution of angiographic diameter stenosis and physiological indexes is shown in Figure 2.

Correlation and agreement between μ QFR and FFR

There was a good correlation between μ QFR and FFR for both none/mildly (Spearman's $\rho = 0.768$; $p < 0.001$) and moderately/severely (Spearman's $\rho = 0.760$; $p < 0.001$) calcified coronary arteries (Fig. 3A, B), with no significant difference between the two correlation coefficients (z-statistic = 0.152, $p = 0.879$). A Bland-Altman analysis also showed a good agreement between μ QFR and FFR for both none/mildly (mean difference = 0.009 ± 0.053) and moderately/severely (mean difference = 0.005 ± 0.056) calcified coronary arteries (Fig. 3C, D).

μ QFR and angiography for detecting functionally significant lesions in different calcification groups

As shown in Figure 4, high discriminatory power was demonstrated by receiver-operating

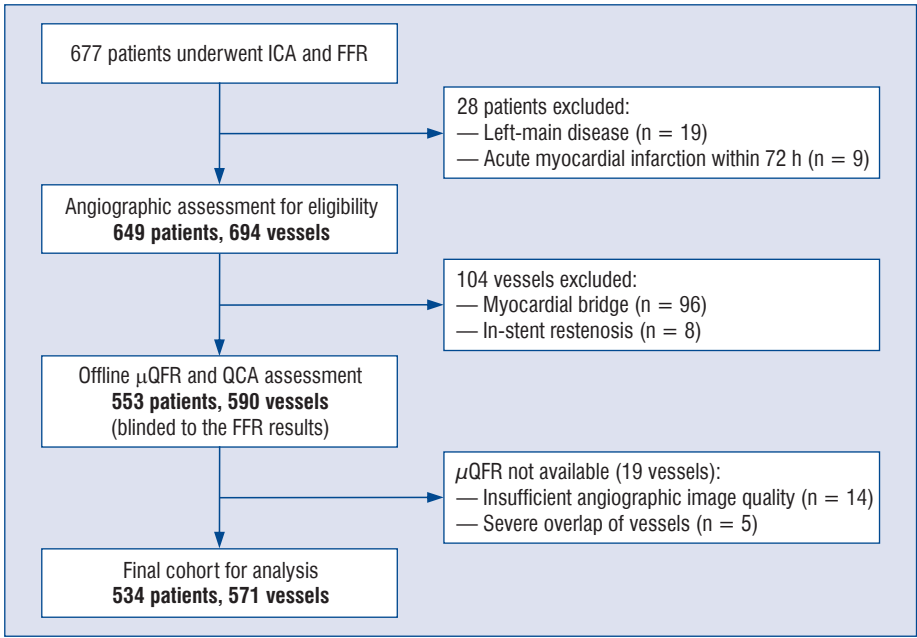


Figure 1. Flow diagram of patient selection; μ QFR — Murray law-based quantitative flow ratio; FFR — fractional flow reserve; ICA — invasive coronary angiography; QCA — quantitative coronary angiography.

Table 1. Baseline characteristics of included patients stratified by quantity of calcium.

Variables	Quantity of calcium		P
	None or mild (n = 461)	Moderate or severe (n = 73)	
Age [years]	65.7 ± 10.1	68.9 ± 8.8	0.012
Male	307 (66.6)	52 (71.2)	0.433
BMI [kg/m ²]	25.2 ± 3.4	23.8 ± 3.3	0.002
Systolic pressure [mmHg]	137.2 ± 19.1	134.8 ± 18.6	0.323
Diastolic pressure [mmHg]	79.1 ± 11.8	77.9 ± 11.1	0.391
Hypertension	345 (74.8)	57 (78.1)	0.550
Diabetes mellitus	131 (28.4)	19 (26.0)	0.673
Dyslipidemia	218 (47.3)	35 (47.9)	0.917
Current smoker	150 (32.5)	26 (35.6)	0.603
Prior MI	39 (8.5)	7 (9.6)	0.749
Prior PCI	110 (23.9)	23 (31.5)	0.160
Multivessel disease	253 (54.9)	59 (80.8)	< 0.001
Clinical symptoms:			1.000
Stable angina	397 (86.1)	64 (87.7)	
Unstable angina	55 (11.9)	8 (11.0)	
NSTEMI	9 (2.0)	1 (1.4)	

Values are given as mean ± standard deviation or number (%); BMI — body mass index; MI — myocardial infarction; NSTEMI — non-ST-segment elevation myocardial infarction; PCI — percutaneous coronary intervention

characteristics curve analysis in both none/mildly and moderately/severely calcified arteries with no statistically significant difference (AUC: 0.91, 95% CI: 0.88–0.93 vs. AUC: 0.87, 95% CI: 0.78–0.94,

p = 0.421). Per-vessel diagnostic parameters of μ QFR among different calcification subgroups are shown in Table 3. No significant difference was found for μ QFR in both sensitivity (0.70 vs.

Table 2. Lesion characteristics stratified by quantity of calcium.

Variables	Quantity of calcium		P
	None or mild (n = 496)	Moderate or severe (n = 75)	
Interrogated vessels:			0.226
LAD	331 (66.7)	56 (74.7)	
LCX	84 (16.9)	7 (9.3)	
RCA	81 (16.3)	12 (16.0)	
Lesion location:			0.054
Proximal	243 (49.0)	46 (61.3)	
Middle	220 (44.4)	28 (37.3)	
Distal	33 (6.7)	1 (1.7)	
QCA parameters:			
QCA-DS [%]	37.8 \pm 8.4	39.8 \pm 7.3	0.043
MLD [mm]	1.81 (1.54, 2.17)	1.77 (1.52, 2.10)	0.419
Lesion length [mm]	19.3 (11.7, 30.2)	24.9 (16.7, 34.4)	0.002
Tandem lesions	56 (11.3)	12 (16.0)	0.241
FFR	0.87 (0.81, 0.91)	0.81 (0.77, 0.86)	< 0.001
FFR \leq 0.80	114 (23.0)	36 (48.0)	< 0.001
μ QFR	0.89 (0.82, 0.93)	0.83 (0.76, 0.89)	< 0.001
μ QFR \leq 0.80	104 (21.0)	29 (38.7)	0.001

Values are given as mean \pm standard deviation or median (25th–75th percentiles) or number (%); μ QFR — Murray law-based quantitative flow ratio; FFR — fractional flow reserve; LAD — left anterior descending artery; LCX — left circumflex; MLD — minimum lumen diameter; QCA — quantitative coronary angiography; QCA-DS — quantitative coronary angiographic diameter stenosis; RCA — right coronary artery

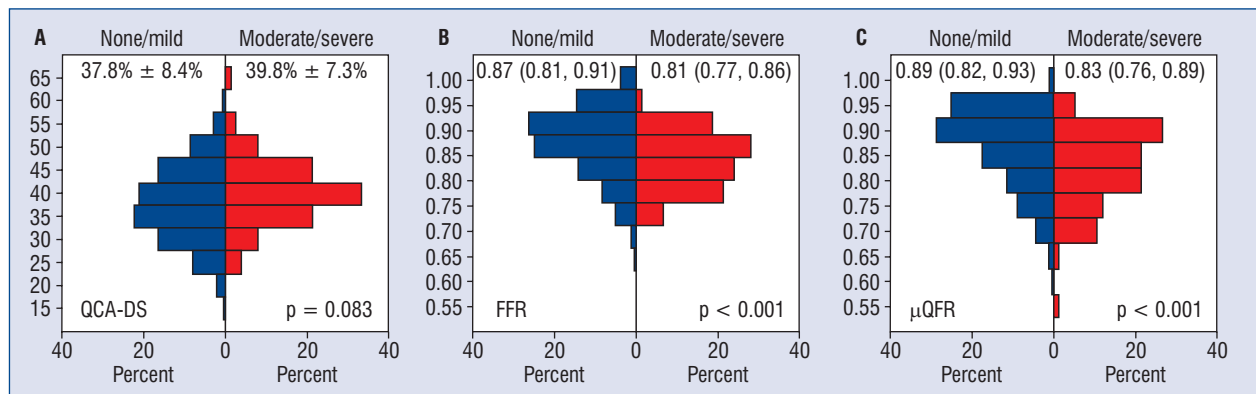


Figure 2. Distribution of angiographic diameter stenosis and physiological indices. There was no significant difference in the distribution of quantitative coronary angiographic diameter stenosis (QCA-DS) (A) according to calcification whereas significant difference existed in the distribution of fractional flow reserve (FFR) (B) and Murray law-based quantitative flow ratio (μ QFR) (C) between the two calcification groups. Values are given as mean \pm standard deviation or median (25th–75th percentiles).

0.69, $p = 0.861$) and specificity (0.94 vs. 0.90, $p = 0.192$) between the two groups whereas there was a relatively higher proportion of overall μ QFR-FFR discordance among vessels with moderate or severe calcification (20.5% vs. 12.0%, $p = 0.045$). On a per-vessel level, μ QFR exhibited superior discrimination to QCA-DS and lesion

length for detecting functionally significant lesions, regardless of the degree of calcification (Fig. 4).

To exclude the influence of confounding factors on the relationship between diagnostic accuracy and calcification, a multivariable analysis was performed by entering both calcification and baseline variables that might be associated with μ QFR-FFR

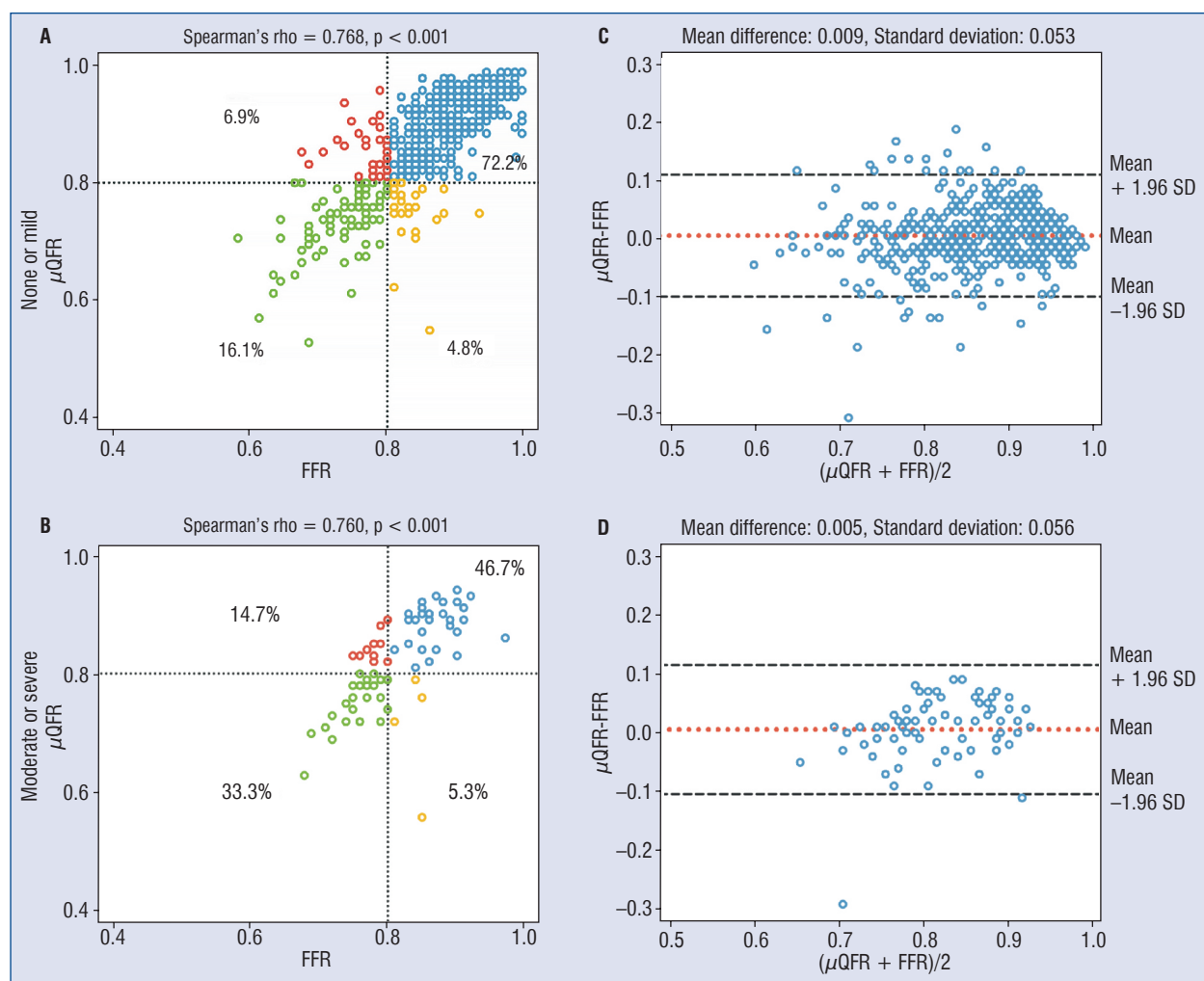


Figure 3. The correlation and agreement between Murray-law based quantitative flow ratio (μ QFR) and invasive fractional flow reserve (FFR); **A, B.** μ QFR showed a significant correlation with FFR regardless of calcification severity. μ QFR-FFR discordance occurred in 11.7% and 20.0% of vessels with none/mild and moderate/severe calcification, respectively; **C, D.** Bland-Altman plots showed that there was a good agreement between μ QFR and FFR in both two calcification categories.

discordance into the model (**Suppl. Table S1**). The results showed that dyslipidemia, QCA-DS, and lesion length were independently associated with overall μ QFR-FFR discordance whereas the presence of moderate or severe calcification (adjusted odds ratio [OR]: 1.529, 95% CI: 0.788–2.968, $p = 0.210$) was not responsible for the misclassification of μ QFR (Table 4). A representative case of μ QFR and angiography with FFR is shown in Figure 5.

Discussion

In this study, the diagnostic performance of μ QFR in coronary arteries with different degrees

of calcification was investigated, using invasive FFR as the reference standard. Results showed that μ QFR, the latest generation of AI-assisted hydrodynamic algorithm for angiographic images, had a good accuracy to identify functional ischemia in angiographically intermediate coronary lesions and this robust performance was not significantly influenced by the quantity of calcium. Furthermore, μ QFR provided an incremental value over conventional angiography alone for the physiological assessment of coronary lesions in both calcified and non-calcified coronary arteries.

Coronary calcification is a challenge for imaging-derived FFR simulation because it may potentially compromise the recognition of vascu-

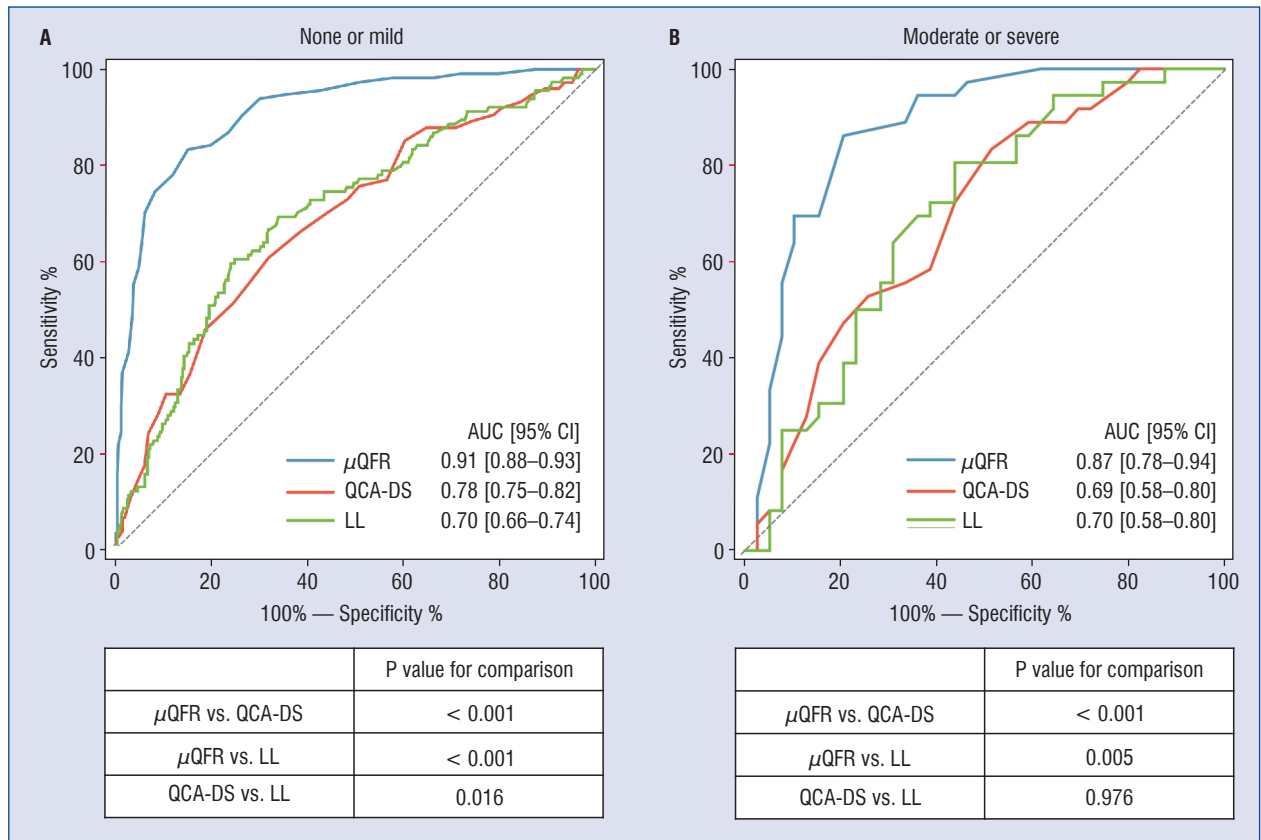


Figure 4. The per-vessel receiver characteristic operating curves of Murray-law based quantitative flow ratio (μ QFR) and quantitative coronary angiographic-derived parameters for identifying functional ischemia. In both vessels with none/mild (A) and moderate/severe (B) calcification, μ QFR showed a higher discrimination for functional ischemia than quantitative coronary angiographic diameter stenosis (QCA-DS) and lesion length (LL); AUC — area under the receiver-operating curve; CI — confidence interval.

Table 3. Per-vessel diagnostic performance of μ QFR stratified by quantity of calcium.

	Quantity of calcium	
	None or mild	Moderate or severe
Overall population	N = 496	N = 75
Accuracy	0.88 (0.85–0.91)	0.80 (0.69–0.88)
Sensitivity	0.70 (0.61–0.78)	0.69 (0.52–0.84)
Specificity	0.94 (0.91–0.96)	0.90 (0.76–0.97)
PPV	0.77 (0.69–0.83)	0.86 (0.71–0.94)
NPV	0.91 (0.89–0.93)	0.76 (0.66–0.84)

Values are given as n with corresponding 95% confidence intervals. Positive test results are defined as μ QFR \leq 0.80 with invasive fractional flow reserve \leq 0.80 as the reference standard; μ QFR — Murray law-based quantitative flow ratio; QCA-DS — quantitative coronary angiographic diameter stenosis; NPV — negative predictive value; PPV — positive predictive value

lar lumen and the drawing of arterial shape [15]. However, the specific impact of calcium deposits on the accuracy of AI-assisted μ QFR is not well understood. According to available research, this is the first study to examine the performance of

μ QFR in coronary arteries with and without calcification. Herein, results suggested that μ QFR provided high and incremental diagnostic value than angiography alone for the detection of functional ischemia regardless of calcium burden, which

Table 4. Adjustment of confounding factors in the relationship between calcification and overall μ QFR-FFR discordance.

	Adjusted OR (95% CI)	P
Male	0.829 (0.416–1.653)	0.594
Dyslipidemia	1.819 (1.062–3.115)	0.029
Current smoking	1.386 (0.781–2.461)	0.265
Prior PCI	1.690 (0.962–2.971)	0.068
Multivessel disease	1.161 (0.632–2.136)	0.630
QCA-DS, 10%	1.719 (1.221–2.419)	0.002
Lesion length, 10 mm	1.338 (1.100–1.626)	0.003
Moderate/severe calcification	1.529 (0.788–2.968)	0.210

The multivariate logistic regression model was performed using the enter method to include all covariates; μ QFR — Murray law-based quantitative flow ratio; CI — confidence interval; FFR — fractional flow reserve; MLD — minimum lumen diameter; OR — odds ratio; PCI — percutaneous coronary intervention; QCA-DS — quantitative coronary angiographic diameter stenosis

is similar to previous findings on FFR derived from coronary computed tomography angiography (CT-FFR) [16–18]. A recent post hoc analysis of the FAST-FFR (FFR_{angio} Accuracy versus Standard FFR) study also confirmed that calcification did not affect the sensitivity or specificity of FFR derived from coronary angiography [19]. This phenomenon might be explained by the complexity of the hemodynamic numerical simulation. The computation of μ QFR is not only based on combined geometrical data but also includes contrast flow velocity [20], which means that calcification is only involved a small part of this process.

Theoretically, arterial intimal calcification could protrude into the coronary lumen, resulting in vascular stenosis and subsequently reduced blood flow [21]. However, calcification might have little effect on intracoronary pressure. Coronary artery calcification was not associated with the pressure gradient before and after the administration

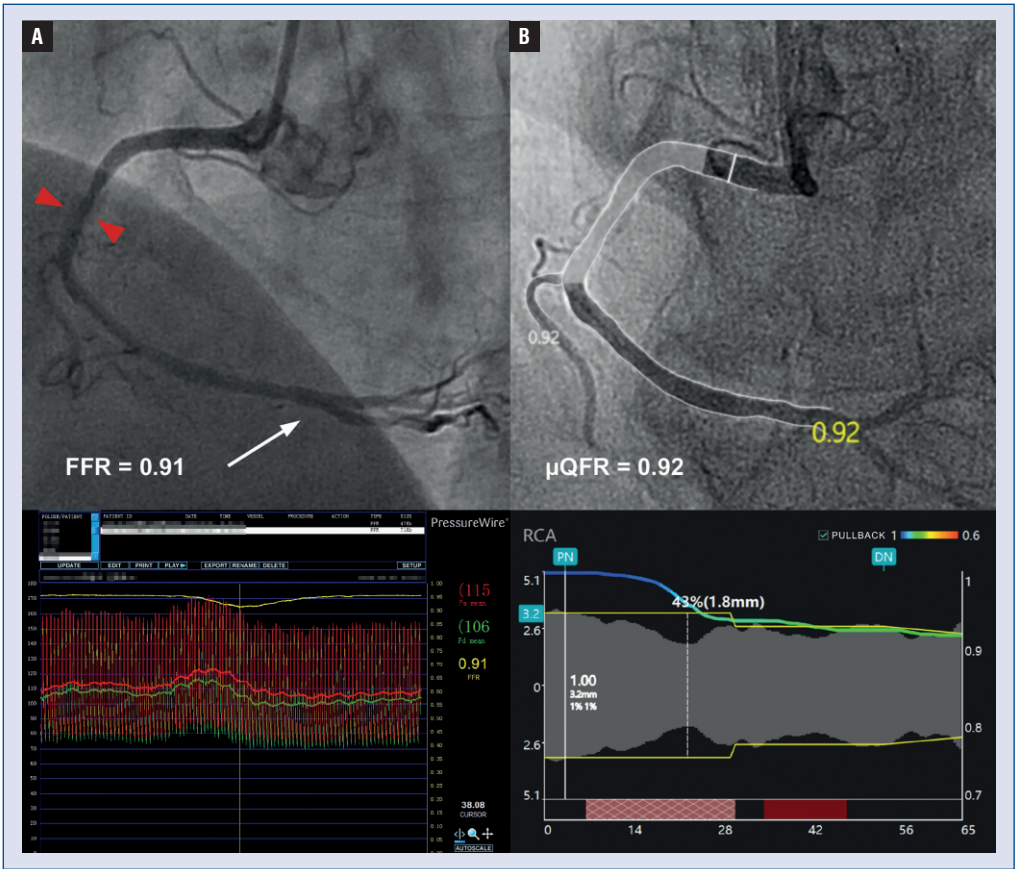


Figure 5. Representative images of Murray-law based quantitative flow ratio (μ QFR) analysis in a severe calcified coronary lesion without functional ischemia; **A.** Coronary angiography shows an intermediate lesion at the proximal segment of the right coronary artery with severe calcification (red arrowhead), with a wire-based fractional flow reserve (FFR) of 0.91; **B.** Artificial-intelligence-assisted quantitative coronary angiography and color-coded μ QFR computation (μ QFR = 0.92).

of adenosine [22]. Lesion length (82%), QCA-DS (64%), and minimum lumen diameter (55%) were reported as the most frequently used variables in the 11 clinical prediction models for FFR whereas calcification was only used in one of them (9%) [23]. Velangi et al. [24] also found that only lesion length and low-attenuation plaque were significant independent predictors of ischemia detected by FFR although spotty calcification was predictive of abnormal FFR on univariate analysis. Interestingly, the association between calcification and overall μ QFR-FFR discordance was abolished when lesion length was included in the multivariable model, suggesting that atherosclerotic burden may have a greater influence on blood flow than calcification. To some extent, calcification may be more a reflection of plaque vulnerability than physiological severity [25]. However, its role in plaque homeostasis still awaits further investigation given its complex relationship with lipids and obesity [26, 27].

Unlike previous studies on CT-FFR [16–18], a slight decline was observed in diagnostic accuracy of μ QFR among vessels with moderate or severe calcification, that is the overall probability that a patient is correctly classified, which reflected the same aspect as μ QFR-FFR discordance. Considering that this value is highly dependent on disease prevalence [28], the relationship was further evaluated between calcification and μ QFR-FFR discordance to eliminate the influence of confounding factors. By multivariable analysis, the presence of moderate or severe calcification was not associated with μ QFR-FFR discordance after adjustment for age, multi-vessel disease, lesion location, and lesion length. Furthermore, only a small proportion of vessels was not eligible for μ QFR computation due to suboptimal image quality (none due to severe calcification). These findings further support the present hypothesis that AI-assisted μ QFR may overcome the influence of calcification on fluoroscopic images with superior performance to angiography alone, thereby probably improving the clinical decision-making and outcomes for patients with coronary artery disease. However, it was noted that a conventional threshold (μ QFR \leq 0.80 or QCA-DS \geq 50%) may impair their diagnostic performance for detection of functional ischemia in such a population with less calcification and atherosclerotic burden. Therefore, the cutoff of μ QFR needs to be further refined according to the severity of calcification and stenosis.

Limitations of the study

There are several limitations that should be addressed. Firstly, a retrospective, single-center

design may increase the susceptibility to bias despite a relatively large population. To avoid the influence of subjective factors, angiographic images were blinded when reviewed. Secondly, coronary calcification was determined based on angiography rather than intravascular ultrasound which is more sensitive to evaluating the burden and morphology of calcium. Finally, there was a relatively low prevalence of severe vascular calcification in the present study, although this represented the real-world situation. Large, multicenter, prospective studies are still warranted to validate the current findings in a broad spectrum of participants.

Conclusions

In conclusion, AI-assisted μ QFR demonstrated high discrimination of hemodynamically significant coronary lesions regardless of calcium burden. In the setting of coronary calcification, μ QFR can still provide incremental value over angiography alone for the physiological assessment of coronary lesions. Further randomized studies are necessary to determine the optimum threshold for μ QFR-guided strategy and its impact on clinical outcomes in patients with severe coronary calcification.

Acknowledgments

This work was supported by the Jiangsu Provincial Key Research and Development Program (BE2022852), the Jiangsu Provincial Key Medical Discipline (ZDXKA2016023), and the National Natural Science Foundation of China (81870213 and 82070295).

Conflict of interest: Shengxian Tu received research grants from Pulse Medical Imaging Technology. Other authors report no conflicts of interest regarding this manuscript.

References

1. Tonino PAL, Bruyne BDe, Pijls N, et al. Fractional flow reserve versus angiography for guiding percutaneous coronary intervention. *N Engl J Med*. 2009; 360(3): 213–224, doi: [10.1056/nejmoa0807611](https://doi.org/10.1056/nejmoa0807611), indexed in Pubmed: [19144937](https://pubmed.ncbi.nlm.nih.gov/19144937/).
2. De Bruyne B, Fearon W, Pijls N, et al. Fractional flow reserve-guided PCI for stable coronary artery disease. *N Engl J Med*. 2014; 371(13): 1208–1217, doi: [10.1056/nejmoa1408758](https://doi.org/10.1056/nejmoa1408758), indexed in Pubmed: [25176289](https://pubmed.ncbi.nlm.nih.gov/25176289/).
3. Dehmer GJ, Weaver D, Roe MT, et al. A contemporary view of diagnostic cardiac catheterization and percutaneous coronary intervention in the United States: a report from the CathPCI Registry of the National Cardiovascular Data Registry, 2010 through June 2011. *J Am Coll Cardiol*. 2012; 60(20): 2017–2031, doi: [10.1016/j.jacc.2012.08.966](https://doi.org/10.1016/j.jacc.2012.08.966), indexed in Pubmed: [23083784](https://pubmed.ncbi.nlm.nih.gov/23083784/).

4. Tu S, Westra J, Adgedj J, et al. Fractional flow reserve in clinical practice: from wire-based invasive measurement to image-based computation. *Eur Heart J*. 2020; 41(34): 3271–3279, doi: [10.1093/eurheartj/ehz918](#), indexed in Pubmed: [31886479](#).
5. Xu Bo, Tu S, Qiao S, et al. Diagnostic accuracy of angiography-based quantitative flow ratio measurements for online assessment of coronary stenosis. *J Am Coll Cardiol*. 2017; 70(25): 3077–3087, doi: [10.1016/j.jacc.2017.10.035](#), indexed in Pubmed: [29101020](#).
6. Jelmer W, Krogsgaard AB, Gianluca C, et al. Diagnostic performance of in-procedure angiography-derived quantitative flow reserve compared to pressure-derived fractional flow reserve: the FAVOR II Europe-Japan study. *J Am Heart Assoc*. 2018; 7(14): e009603, doi: [10.1161/JAHA.118.009603](#), indexed in Pubmed: [29980523](#).
7. Westra J, Tu S, Winther S, et al. Evaluation of coronary artery stenosis by quantitative flow ratio during invasive coronary angiography: the WIFI II study (Wire-Free Functional Imaging II). *Circ Cardiovasc Imaging*. 2018; 11(3): e007107, doi: [10.1161/CIRCIMAGING.117.007107](#), indexed in Pubmed: [29555835](#).
8. Tu S, Ding D, Chang Y, et al. Diagnostic accuracy of quantitative flow ratio for assessment of coronary stenosis significance from a single angiographic view: A novel method based on bifurcation fractal law. *Catheter Cardiovasc Interv*. 2021; 97 Suppl 2: 1040–1047, doi: [10.1002/ccd.29592](#), indexed in Pubmed: [33660921](#).
9. Karacsonyi J, Karmaliotis D, Alaswad K, et al. Impact of calcium on chronic total occlusion percutaneous coronary interventions. *Am J Cardiol*. 2017; 120(1): 40–46, doi: [10.1016/j.amjcard.2017.03.263](#), indexed in Pubmed: [28499595](#).
10. Zuo W, Sun R, Zhang X, et al. The association between quantitative flow ratio and intravascular imaging-defined vulnerable plaque characteristics in patients with stable angina and non-ST-segment elevation acute coronary syndrome. *Front Cardiovasc Med*. 2021; 8: 690262, doi: [10.3389/fcvm.2021.690262](#), indexed in Pubmed: [34277736](#).
11. Zuo W, Zhang X, Carvalho A, et al. Impact of diabetes mellitus on the relationship between a Poiseuille-based index and fractional flow reserve in intermediate coronary lesions. *Coron Artery Dis*. 2021; 32(7): 632–638, doi: [10.1097/MCA.0000000000001024](#), indexed in Pubmed: [33534242](#).
12. Hinkle D, Wiersma W, Jurs S. *Applied statistics for the behavioral sciences*. 2nd ed. Houghton Mifflin Company, Boston 1988.
13. Richardson JTE. The analysis of 2×2 contingency tables — yet again. *Stat Med*. 2011; 30(8): 890; author reply 891–890; author reply 892, doi: [10.1002/sim.4116](#), indexed in Pubmed: [21432882](#).
14. DeLong ER, DeLong DM, Clarke-Pearson DL. Comparing the areas under two or more correlated receiver operating characteristic curves: a nonparametric approach. *Biometrics*. 1988; 44(3): 837–845, indexed in Pubmed: [3203132](#).
15. Dey D, Lin A. Machine-Learning CT-FFR and extensive coronary calcium: overcoming the Achilles heel of coronary computed tomography angiography. *JACC Cardiovasc Imaging*. 2020; 13(3): 771–773, doi: [10.1016/j.jcmg.2019.08.011](#), indexed in Pubmed: [31542540](#).
16. Nørgaard BL, Gaur S, Leipsic J, et al. Influence of coronary calcification on the Diagnostic performance of CT angiography derived FFR in coronary artery disease: a substudy of the NXT trial. *JACC Cardiovasc Imaging*. 2015; 8(9): 1045–1055, doi: [10.1016/j.jcmg.2015.06.003](#), indexed in Pubmed: [26298072](#).
17. Tesche C, Otani K, De Cecco CN, et al. Influence of coronary calcium on diagnostic performance of machine learning CT-FFR: results from MACHINE registry. *JACC Cardiovasc Imaging*. 2020; 13(3): 760–770, doi: [10.1016/j.jcmg.2019.06.027](#), indexed in Pubmed: [31422141](#).
18. Di Jiang M, Zhang XL, Liu H, et al. The effect of coronary calcification on diagnostic performance of machine learning-based CT-FFR: a Chinese multicenter study. *Eur Radiol*. 2021; 31(3): 1482–1493, doi: [10.1007/s00330-020-07261-2](#), indexed in Pubmed: [32929641](#).
19. Kobayashi Y, Collet C, Achenbach S, et al. Diagnostic performance of angiography-based fractional flow reserve by patient and lesion characteristics. *EuroIntervention*. 2021; 17(4): e294–e300, doi: [10.4244/EIJ-D-19-00933](#), indexed in Pubmed: [32364503](#).
20. Tu S, Westra J, Yang J, et al. Diagnostic accuracy of fast computational approaches to derive fractional flow reserve from diagnostic coronary angiography: the international multicenter FAVOR pilot study. *JACC Cardiovasc Interv*. 2016; 9(19): 2024–2035, doi: [10.1016/j.jcin.2016.07.013](#), indexed in Pubmed: [27712739](#).
21. Yu M, Li Y, Li W, et al. Calcification remodeling index assessed by cardiac CT predicts severe coronary stenosis in lesions with moderate to severe calcification. *J Cardiovasc Comput Tomogr*. 2018; 12(1): 42–49, doi: [10.1016/j.jcct.2017.09.017](#), indexed in Pubmed: [28988831](#).
22. Borren NM, Ottervanger JP, Mouden M, et al. Influence of coronary calcification on hyperemic response during fractional flow reserve measurements. *Int J Cardiol*. 2019; 285: 93–96, doi: [10.1016/j.ijcard.2019.02.037](#), indexed in Pubmed: [30857847](#).
23. Zuo W, Zhang R, Yang M, et al. Clinical prediction models of fractional flow reserve: an exploration of the current evidence and appraisal of model performance. *Quant Imaging Med Surg*. 2021; 11(6): 2642–2657, doi: [10.21037/qims-20-1274](#), indexed in Pubmed: [34079730](#).
24. Velangi PS, Maharaj V, Athwal SS, et al. Computed tomography coronary plaque characteristics predict ischemia detected by invasive fractional flow reserve. *J Thorac Imaging*. 2021; 36(6): 360–366, doi: [10.1097/RTI.0000000000000543](#), indexed in Pubmed: [32701769](#).
25. Shi X, Gao J, Lv Q, et al. Calcification in atherosclerotic plaque vulnerability: friend or foe? *Front Physiol*. 2020; 11: 56, doi: [10.3389/fphys.2020.00056](#), indexed in Pubmed: [32116766](#).
26. Hsu JJ, Tintut Y, Demer LL. Lipids and cardiovascular calcification: contributions to plaque vulnerability. *Curr Opin Lipidol*. 2021; 32(5): 308–314, doi: [10.1097/MOL.0000000000000777](#), indexed in Pubmed: [34320564](#).
27. Kovacic JC, Lee P, Baber U, et al. Inverse relationship between body mass index and coronary artery calcification in patients with clinically significant coronary lesions. *Atherosclerosis*. 2012; 221(1): 176–182, doi: [10.1016/j.atherosclerosis.2011.11.020](#), indexed in Pubmed: [22204865](#).
28. Akobeng AK. Understanding diagnostic tests 1: sensitivity, specificity and predictive values. *Acta Paediatr*. 2007; 96(3): 338–341, doi: [10.1111/j.1651-2227.2006.00180.x](#), indexed in Pubmed: [17407452](#).